
REAL-TIME LIGHTWEIGHT GAZE PRIVACY-PRESERVATION TECHNIQUES VALIDATED VIA OFFLINE GAZE-BASED INTERACTION SIMULATION

Mehedi Hasan Raju*
Texas State University
San Marcos, Texas, USA
m.raju@txstate.edu

Oleg V. Komogortsev
Texas State University
San Marcos, Texas, USA
ok11@txstate.edu

ABSTRACT

This study examines the effectiveness of the real-time privacy-preserving techniques through an offline gaze-based interaction simulation framework. Those techniques aim to reduce the amount of identity-related information in eye-tracking data while improving the efficacy of the gaze-based interaction. Although some real-time gaze privatization methods were previously explored, their validation on the large dataset was not conducted. We propose a functional framework that allows to study the efficacy of real-time gaze privatization on an already collected offline dataset. The key metric used to assess the reduction of identity-related information is the identification rate, while improvements in gaze-based interactions are evaluated through signal quality during interaction. Our additional contribution is the employment of an extremely lightweight Kalman filter framework that reduces the amount of identity-related information in the gaze signal and improves gaze-based interaction performance.

Keywords Gaze-interaction, Privacy, Filtering, Real-time, Virtual Reality

1 INTRODUCTION

Eye-tracking has become an integral component of extended reality (XR) technologies, including virtual and augmented reality [1, 2]. It is now featured in consumer devices² that exemplify the growing integration of gaze data within immersive systems across consumer and research domains [3]. Gaze data enable intuitive, gaze-based interaction [4] and serve as a rich source of information for diverse applications, including foveated rendering [5, 6], healthcare [7, 8], neuroscience [9, 10], education [11], gaming [12], etc. Moreover, gaze data also contain person-specific signatures that can be used in biometric authentication [13, 14, 15] and user identification [16, 17, 18], raising critical concerns about data privacy and potential misuse.

Although researchers often anonymize datasets by removing explicit identifiers such as names, birth dates, or gender before making them publicly available, studies have shown that individuals can still be re-identified from gaze data alone (53 of 58 subjects are correctly identified in [13]). As eye-tracking becomes increasingly embedded in consumer devices, ensuring privacy preservation has become more critical than ever. With gaze data now central to many applications, achieving a balance between privacy preservation and user experience is essential to promote user trust in gaze-based technologies. To address this risk, researchers are actively developing privacy-preserving techniques aimed at safeguarding users while maintaining the utility of gaze data.

Current privacy measures prevent re-identification by restricting access to raw gaze data through API design [19], but this also limits some of the above-mentioned critical applications like foveated rendering or gaze prediction [20]. Therefore, to fully explore the potential of eye-tracking across multiple applications, access to raw data cannot be entirely restricted. Prior work has proposed privacy-preserving techniques that perturb eye-movement data to reduce

*corresponding author

²<https://about.meta.com/realitylabs/orion>, <https://www.apple.com/apple-vision-pro>

re-identification risk and protect user privacy [21]. Generally, these methods demonstrate strong effectiveness in preserving privacy for specific applications. However, most of the existing techniques have been evaluated without considering their impact on interaction performance or system usability, leaving open the question of how privacy-preserving techniques perform in gaze-based interaction pipelines.

In this study, we focus on gaze-based interaction as the primary application area, emphasizing the spatial accuracy of gaze data during interaction as a measure of utility. Our methodology closely follows the offline gaze-based interaction simulation pipeline proposed by [3]. Building on this framework, we aim to evaluate how lightweight real-time privacy-preserving techniques applied to gaze data can reduce re-identification risk while improving interaction performance, represented by spatial accuracy. It is important that while offline evaluation is employed, we do not foresee any issues with the implementation and employment of the methods that we propose here in an actual on-device gaze-driven interaction, including gaze and pinch. Additionally, the dataset that we employ for evaluation is not recorded in a course of actual gaze-based interaction, but it provides a reasonable approximation via a random saccade task stimulus, where a subject is tasked to follow a jumping target as closely as possible. The strength of our technique is that it allows to show the efficacy of both real-time privatization and improvements in gaze interaction performance on a large pool of subjects, providing a broader statistical foundation that is typically difficult to achieve with interaction-based datasets.

The core question guiding our research is *Can real-time lightweight privacy-preserving techniques be integrated into a gaze-based interaction pipeline to mitigate re-identification risk while improving system usability?* To address our research question and advance understanding in real-time gaze-based privacy preservation, this paper presents the following key contributions:

1. Real-time implementation of multiple privacy-preserving techniques and evaluating them in the context of real-time interaction scenarios to mitigate privacy risk.
2. Evaluation of the impact of lightweight real-time privacy-preserving techniques on utility, as measured by spatial accuracy.
3. Measurement and analysis of additional latency introduced by the implemented techniques during real-time operation.

2 BACKGROUND AND PRIOR WORK

Eye movements have long been recognized as a potential biometric modality. Kasprowski and Ober’s seminal study first established the feasibility of using eye movements for user authentication [22]. Since then, research has advanced significantly in both user identification and verification [23, 24, 25, 26, 27, 28, 17, 18]. Recent developments, particularly deep learning-based methods, have achieved state-of-the-art performance in gaze-based user identification [13, 15]. Beyond explicit identification, gaze patterns can also reveal implicit user characteristics. Prior studies show that gaze data encode both physical attributes (e.g., age, gender, ethnicity) and behavioral traits (e.g., personality, cognitive states, emotional responses) [29, 30, 31, 32, 33]. Sensitive factors such as sexual preference, hormonal cycles, and mental activities can also be inferred with the above random accuracy. These findings establish that gaze data can unintentionally disclose identifiable and sensitive personal information, posing privacy risks. So, gaze data should be protected through both policy frameworks and robust data protection strategies [34, 29].

Various methods of person identification based on the eye tracking techniques have been introduced during the last few years [35]. However, conventional de-identification approaches do not fully guarantee privacy, as correlated datasets can still be used to infer personal information.

Bozkir et al. [36] proposed a privacy-preserving framework based on randomized encoding, allowing a regression model to be trained privately using synthetic eye images to estimate gaze. Nevertheless, such de-identification typically removes only explicit identifiers from database entries while leaving underlying sensitive information potentially exposed [37]. Furthermore, anonymization is vulnerable to statistical de-anonymization attacks [38].

More recently, differential privacy (DP) has emerged as an effective approach for privatizing gaze data. Liu et al. [39] introduced two noise-injection mechanisms that guarantee privacy and systematically analyze the privacy-utility trade-off. By applying DP to gaze streams, they protected spatial gaze information within bounds defined by the DP threshold. Similarly, Li et al. [40] applied differential privacy guarantees to raw gaze streams designed to obfuscate users’ gaze behavior. In general, DP achieves privacy by adding noise before data release, thereby reducing inter-user variation and making the detection of sensitive attributes from gaze data more difficult [36, 41]. Most recently, Aziz et al. [42] introduced an autoencoder-based approach that injects noise in the latent space, preserving key physiological characteristics of eye movements while enhancing privacy.

The most relevant prior work on privacy preservation for eye-tracking data involves mechanisms that directly perturb gaze signals—an approach particularly useful for real-world applications that operate on gaze data in its native form [19, 21]. For example, temporal downsampling has been used to lower the sampling rate of collected gaze data [19]; Gaussian noise has been added to raw recordings [19]; linear weighted averaging [21]. Other filtering techniques—such as median filtering [43], Kalman filter [44, 45], and finite impulse response filtering [46]—may also reduce person-specific patterns by smoothing raw gaze data and removing noise that carries identifiable characteristics [14].

Despite these advances, none of the existing techniques have been implemented or evaluated in real-time gaze-based interaction environments with the dual objective of preserving privacy while maintaining utility—measured through interaction spatial accuracy. This study addresses this gap by implementing real-time adaptations of several lightweight but promising approaches and evaluating their performance in terms of both privacy protection and utility.

3 METHODOLOGY

We structured our methodology into three main components: (1) *Data Privatization*, which encompasses the privacy-preserving techniques we have implemented to generate “privatized” gaze data; (2) *Privacy Metric Computation*, where we quantify the level of privacy achieved; and (3) *Utility Measurement*, which evaluates the spatial accuracy of the privatized data through real-time simulations of gaze interactions.

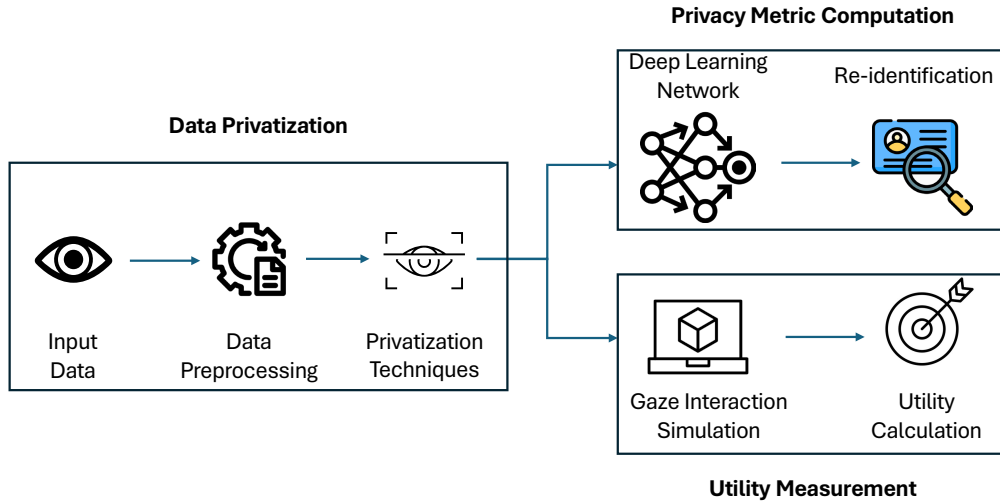


Figure 1: Workflow Diagram of the Methodology.

3.1 Data Privatization

3.1.1 Dataset

We have utilized the publicly available GazeBase dataset [47], collected from 322 college-aged participants, over nine rounds across three years using an EyeLink 1000 eye-tracker at 1000 Hz. Each recording contains horizontal and vertical eye movements in degrees of visual angle (dva). Participants performed seven eye movement tasks, including random saccades (RAN), reading (TEX), fixation (FXS), horizontal saccades (HSS), two video viewing tasks (VD1 and VD2), and a video-gaming task (Balura game, BLG). Each round included two sessions per participant, 20 minutes apart. This study uses the entire dataset for privacy-metric computation and only uses RAN task data from Round 1 for the utility measurement in the methodology.

Although the employed dataset is not interaction-based, it allows for the analysis of data from a large pool of subjects—a scale that is typically difficult to achieve with interaction-based datasets. More details on the dataset and the recording procedure are available in [47].

3.1.2 Data Preprocessing

We excluded (set to Not a Number, NaN) any individual gaze samples where the subjects were viewing beyond the screen dimensions. For GazeBase, the range for the possible horizontal component of the gaze positional value is from

-23.3 to +23.3, whereas the vertical component is from -18.5 to 11.7 dva [14]. Across the dataset, the median data loss is 1.12%, with a standard deviation of 4.47%; the highest observed data loss in a single recording is 48.01%.

3.1.3 Privatization Techniques

We have employed several lightweight privacy-preserving techniques in our study. Figure 2, shows an example of comparing privacy-preserving techniques we employed to privatize the data.

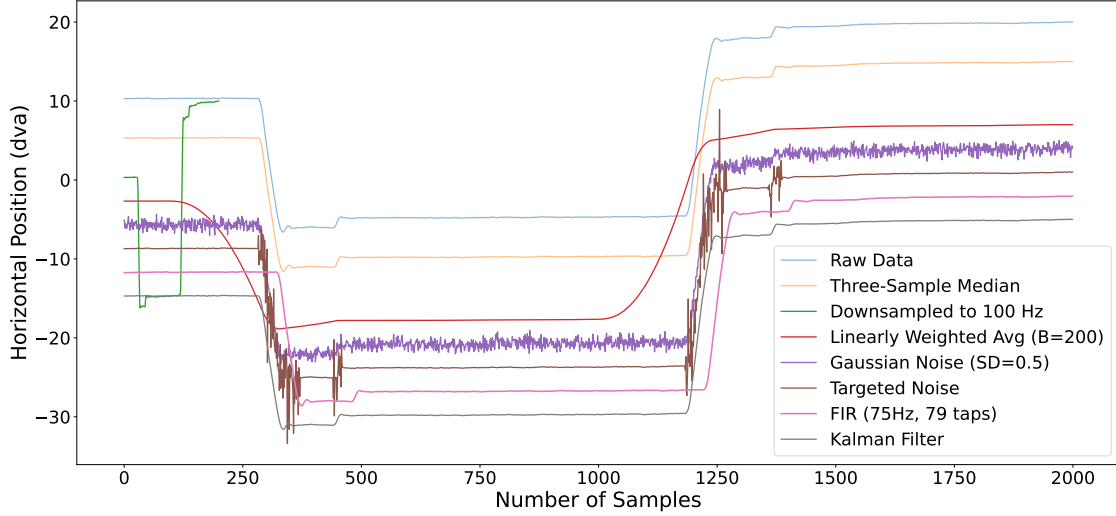


Figure 2: Exemplar comparison of privacy preservation techniques. Each technique is applied to the same two-second segment of raw data. Downsampling reduces the number of samples while preserving the structure of the segment, which is why it ends earlier.

Median Filter To reduce high-frequency noise and remove short-duration artifacts in the recorded gaze coordinates, we implemented a causal three-sample median filter based on [43]. This approach was designed to maintain temporal causality, ensuring that each filtered sample depends only on the current and two preceding observations.

Let x_n denote the raw gaze position at sample n . The causal three-sample median filter computes the output y_n as the median of the three most recent samples:

$$y_n = \text{median}(x_{n-2}, x_{n-1}, x_n). \quad (1)$$

At the start of each sequence, causality is preserved by replicating the first valid sample twice, i.e., $x_{-1} = x_{-2} = x_0$, such that the filter can be applied uniformly from the first sample onward. Missing or invalid gaze samples, typically corresponding to blinks, were handled via forward-filling. Formally, each missing value $x_n = \text{NaN}$ was replaced by the most recent valid sample. If the first sample was missing, it was initialized using the first subsequent valid sample to ensure a consistent starting point.

Because the filter is strictly causal and padded with two copies of the initial sample, it can produce the first output immediately (*initialization* = 0 samples). However, since the output y_n depends on the two preceding samples, the effective temporal alignment corresponds approximately to the median of the window, introducing a fixed *latency* of one sample.

Temporal Downsampling We applied temporal downsampling to the gaze recordings to privatize the data [19]. Temporal downsampling lowers the effective sampling rate of the data by selecting gaze points at regular intervals. This process removes high-frequency temporal information while retaining the general dynamics of eye movements. This procedure effectively reduced the temporal resolution from the original 1000 Hz to several target rates (e.g., 500, 250, 100, ≈ 90 and 50 Hz). By removing finer component of eye-tracking signal, temporal downsampling obscures individual-specific oculomotor patterns that could otherwise serve as biometric information.

Downsampling itself does not introduce latency, as each output sample is taken directly from the corresponding input sample without temporal shifting. At most, an initial offset of $(M-1)$ samples may occur if downsampling begins after the first sample, where M is the downsampling factor (2, 4, 10, 11 and 20); however, this reflects in the initialization.

Gaussian Noise To reduce spatial precision, random noise drawn from a Gaussian distribution with zero mean and variance σ^2 was added independently to both the horizontal and vertical gaze coordinates [13, 19]. Formally, for each sample individual channel: $x' = x + \mathcal{N}(0, \sigma^2)$, $y' = y + \mathcal{N}(0, \sigma^2)$ where (x, y) denote the original gaze positions, (x', y') the noise-perturbed coordinates and \mathcal{N} is the noise representation. In our study, we evaluated multiple noise levels corresponding to variance values of $\sigma^2 = \{0.25, 0.5, 1, 2\}$ to examine how reduced spatial precision privatized the data. Gaussian noise addition does not induce any processing latency.

Linear Weighted Moving Average Smoothing To reduce high-frequency noise in the gaze coordinate data, we applied a smoothing procedure based on a weighted moving average following [21]. For each gaze signal (horizontal x and vertical y), a causal linearly weighted moving average was used over a fixed-size sliding window of B samples ($B = 50, 100, 200$). This approach preserves the eye-tracking signal while attenuating small, rapid fluctuations.

Formally, for a discrete gaze signal $s = [s_1, s_2, \dots, s_N]$, the smoothed signal \tilde{s}_i at time index i was computed as:

$$\tilde{s}_i = \frac{1}{D} \sum_{k=0}^{B-1} (k+1) s_{i-k} \quad \text{for } i \geq B \quad (2)$$

where

$$D = \sum_{k=1}^B k = \frac{B(B+1)}{2} \quad (3)$$

is the normalization constant ensuring that the weighted sum remains within the same numerical range as the input signal.

The weighting coefficients increase linearly from 1 (oldest sample) to B (most recent sample), giving greater emphasis to more recent gaze positions within the smoothing window. At the beginning of each sequence, zero-padding was applied to maintain temporal alignment with the original signal length.

Because the filter is causal and uses zero-padding for the initial window, the first output can be produced immediately (samples required for padding is reflected in initialization). However, due to the asymmetric weighting that emphasizes recent samples, the smoothed signal exhibits an inherent latency corresponding to the centroid of the weighting function. For a window length of B , this effective delay equals approximately $\approx \frac{2(B-1)}{3}$ samples.

Targeted Noise Addition To ensure privacy preservation without utility disturbance, we introduced random perturbations to gaze points using a planar Laplace distribution, inspired by [40]. Instead of adding noise to all gaze data, this method specifically perturbs saccades. First, an angle $\theta \sim \mathcal{U}(0, 2\pi)$ is sampled uniformly to determine the direction of the perturbation. Then, a radius $r \sim \text{Exp}(\lambda)$ is drawn from an exponential distribution to set the displacement magnitude. The resulting offset is computed as $(\Delta x, \Delta y) = (r \cos \theta, r \sin \theta)$ and added to the original gaze coordinates.

Here, $\lambda = \frac{r}{\varepsilon}$ represents the Laplace scale, determined by the spatial radius r and the privacy budget ε . In our configuration ($r=1.5, \varepsilon=0.5$), this yields $\lambda = 3$, corresponding to moderate noise that preserves overall gaze trajectory structure while introducing sufficient stochastic variability for privacy protection.

Fixation samples were left unperturbed to preserve fixation stability, which is critical for downstream utility in our analyses. Noise injection is a stateless, per-sample operation and does not require access to past or future gaze samples. It is to be noted that it requires real-time eye-movement classification.

Causal Finite Impulse Response Filter We applied a causal Finite Impulse Response (FIR) filter to both channels to suppress high-frequency noise while preserving temporal ordering for real-time use based on the insights from [46].

For a low-pass response with cutoff frequency (Hz) [$f_c=10, 25, 75$] at sampling rate of 1000 (Hz) and M taps ($M = 29, 49, 79$), we design the impulse response by centering an ideal sinc at $(M-1)/2$ and applying a Hamming window. The coefficients were normalized so that their sum equals one, ensuring that the filter preserves the overall signal amplitude.

The filter was designed as a low-pass response with a specified cutoff frequency and sampling rate. An ideal sinc function was centered at the middle of the filter window and multiplied by a Hamming window to control sidelobes. We maintain the previous $M-1$ inputs as filter state to process data in fixed-size chunks, producing the same result as strict real-time sample-by-sample convolution. The windowed-sinc FIR is linear phase with a constant latency of $\frac{M-1}{2}$ samples. We use a forward-hold policy to remove NaNs prior to filtering: each missing value is replaced with the most recent valid sample; if the sequence starts with NaNs, the first valid sample initializes the prefix.

Kalman Filter–Based Data Smoothing To obtain a smooth and stable representation of gaze position while preserving the underlying motion dynamics, a Kalman filter was employed. This recursive Bayesian estimator infers the true state of the eye (position and velocity) from noisy measurements by alternating between prediction and update steps.

At each time step k , the system state is defined as

$$\mathbf{x}_k = \begin{bmatrix} x_k \\ \dot{x}_k \end{bmatrix}, \quad \mathbf{y}_k = \begin{bmatrix} y_k \\ \dot{y}_k \end{bmatrix}, \quad (4)$$

where x_k and y_k represent horizontal and vertical gaze positions, and \dot{x}_k, \dot{y}_k their corresponding velocities.

Assuming a constant-velocity model with sampling interval Δt , the state transition is described by

$$\mathbf{A} = \begin{bmatrix} 1 & \Delta t \\ 0 & 1 \end{bmatrix}, \quad \mathbf{x}_{k|k-1} = \mathbf{A}\mathbf{x}_{k-1|k-1} + \mathbf{w}_k, \quad (5)$$

where $\mathbf{w}_k \sim \mathcal{N}(0, \mathbf{Q})$ represents the process noise with covariance matrix \mathbf{Q} . The corresponding prediction of uncertainty is

$$\mathbf{P}_{k|k-1} = \mathbf{A}\mathbf{P}_{k-1|k-1}\mathbf{A}^\top + \mathbf{Q}. \quad (6)$$

The measurement model relates the hidden state to the observed gaze coordinates:

$$z_k = \mathbf{H}\mathbf{x}_k + v_k, \quad \mathbf{H} = [1 \ 0], \quad (7)$$

where $v_k \sim \mathcal{N}(0, R)$ is measurement noise with variance R . The Kalman gain, which determines how strongly the new measurement influences the prediction, is computed as-

$$\mathbf{K}_k = \mathbf{P}_{k|k-1}\mathbf{H}^\top (\mathbf{H}\mathbf{P}_{k|k-1}\mathbf{H}^\top + R)^{-1}. \quad (8)$$

The state and covariance are then updated as

$$\mathbf{x}_{k|k} = \mathbf{x}_{k|k-1} + \mathbf{K}_k (z_k - \mathbf{H}\mathbf{x}_{k|k-1}), \quad (9)$$

$$\mathbf{P}_{k|k} = (\mathbf{I} - \mathbf{K}_k\mathbf{H})\mathbf{P}_{k|k-1}. \quad (10)$$

Separate filters were applied to the horizontal and vertical gaze components. For missing or invalid samples (NaN values), only the prediction step was executed, allowing the state estimate to propagate without discontinuity. The process noise covariance \mathbf{Q} and measurement noise R were tuned empirically to balance smoothness and responsiveness: larger process noise increases responsiveness during saccades, whereas larger measurement noise produces smoother estimates during fixations. The resulting filtered trajectories exhibit substantially reduced jitter compared to raw measurements while preserving genuine eye-movement dynamics.

3.2 Privacy Metric Computation

3.2.1 Data Preprocessing and Embedding Generation

Raw gaze signals were processed to derive horizontal and vertical velocity channels using an instantaneous velocity calculation. The data were segmented into non-overlapping 5 seconds windows (5000 samples each) for analysis. Velocities were clamped between $\pm 1000^\circ/\text{s}$ to mitigate noise, z-score normalized across all subjects and segments, and any NaN values were replaced with 0 following [48, 13].

3.2.2 Model Architecture, Training and Evaluation

We have adopted the Eye Know You Too (EKYT) architecture [13], a DenseNet-based [49] model. EKYT comprises 8 convolutional layers with dense connectivity, followed by global average pooling and a fully connected layer that outputs a 128-dimensional embedding. The model was trained using data from Rounds 1–5 (excluding the BLG task). 59 subjects of Round 1 (subjects same as Round 6) were held out for evaluation. The remaining participants ($N = 263$) were split into four non-overlapping folds for cross-validation, ensuring class-balanced distribution [48]. Each fold trained an independent model using the Adam optimizer with OneCycleLR cosine annealing [50, 51], and multi-similarity loss [52] implemented via PyTorch Metric Learning [53]. Each model used 2-channel (horizontal, vertical

velocity) 5000-step inputs, batch size 64 (8 classes \times 8 samples/class), and trained 100 epochs. The final biometric assessment was based solely on the RAN recordings. To maintain consistency with utility measures, we opted for the RAN task. To generate embeddings for each window in both the enrollment and authentication sets, we use the four models that were trained using a 4-fold cross-validation approach. We computed a 128-dimensional embedding for each model and concatenated them to create a single 512-dimensional embedding for each window. This effectively treats the four models as a single ensemble model. Full details about the network architecture, training and evaluation is based on [13].

3.2.3 Privacy Metric: Rank-1 Identification Rate

Rank-1 Identification Rate (Rank-1 IR) is a widely accepted metric in biometric identification and privacy evaluation because it directly reflects the system’s ability to distinguish individuals based on their eye-movement embeddings [13, 21]. A higher Rank-1 IR indicates stronger identifiability and, consequently, lower privacy preservation. In this context, the metric serves as a privacy indicator, where a lower Rank-1 IR implies higher privacy through reduced identifiability from gaze embeddings.

This metric quantifies the proportion of probe (authentication) samples whose most similar enrollment (gallery) sample corresponds to the same individual. Let $\mathbf{S} \in \mathbb{R}^{M \times N}$ denote the similarity matrix between M enrollment and N authentication samples, where each entry S_{ij} represents the similarity score between enrollment sample i and authentication sample j . A corresponding binary matrix \mathbf{Y} encodes ground-truth subject matches, such that $Y_{ij} = 1$ if both samples belong to the same participant and 0 otherwise. For each authentication sample j , the enrollment indices are sorted in descending order of similarity, and the top-ranked match ($i^* = \arg \max_i S_{ij}$) is compared against the true label Y_{i^*j} . The Rank-1 IR is then computed as the mean proportion of correctly identified probes:

$$\text{Rank-1 IR} = \frac{1}{N} \sum_{j=1}^N \mathbb{I}[Y_{i^*j} = 1], \quad (11)$$

where $\mathbb{I}[\cdot]$ is the indicator function. Intuitively, this measure captures the probability that the correct subject is retrieved as the top candidate in the similarity ranking, thereby reflecting overall identification accuracy.

3.3 Utility Measurement

3.3.1 Simulating Real-time Data Stream

We simulate our offline datasets as real-time one following the methodology from [3]. As we are using the offline datasets, we simulate a streaming scenario: reading timestamps and gaze (horizontal and vertical) channels in sequence. We handle missing gaze samples (e.g., NaNs) by forward-filling, assuming real-time data. We then apply eye-movement classification (dispersion-threshold [54], Kalman-filter-based [55]) in real time to classify physiological fixations from the RAN task. The RAN task provides gaze positions and target positions which is required for gaze-interaction simulation using offline datasets. Fixation labeling using the *Friedman-Komogortsev Method (FKM)* [56] served as the ground truth for optimizing parameter settings of the classification algorithms. Parameters yielding the highest agreement with FKM labels were selected as optimal.

IDT: Dispersion threshold = 0.5° and minimum duration = 32 ms.

IKF: chi-square = 3.75, window size = 5, deviation = 1000.

3.3.2 Simulating Gaze-based Interaction

Although the datasets used do not involve interactive gaze behavior, their large participant pools support simulation and enhance generalizability across high-end and consumer devices. We focus on the *RAN* task, which provides gaze positions and target locations. In our simulation, these targets are treated as interactive objects, allowing controlled approximation of gaze-based interaction. We employed Rank-1 Fixation Selection approach from [3] to identify the presumed interaction period. Fixations are detected using the classifications algorithms, with interaction defined by dwell time of 100 ms. For each target, we calculate the Euclidean distance (in dva) between the target and all valid fixations. The fixation with the smallest distance—the *Rank-1 Fixation*—is assumed to represent the intended interaction. No explicit spatial threshold was applied, ensuring inclusivity while emphasizing spatial accuracy. The centroid of the *Rank-1 Fixation* defines the *trigger event*, representing the most probable moment of interaction. In our study, the terms *trigger event* and *interaction* are used interchangeably. Interactions are required to occur within one second of target onset, matching the temporal constraints of the *RAN* task.

3.3.3 Performance Metrics

In our study, we employed the metrics used previously in [3]. We evaluated two key aspects: the effectiveness of the real-time gaze-based interaction simulation methodology in defining interaction, and the associated eye-tracking signal quality. For this component, we have utilized Round 1 data from GazeBase dataset.

Success rate in defining interaction: We quantify the effectiveness of the simulation framework by computing a *success rate*, defined as the ratio of the number of valid interactions to the total possible events (100 targets per recording). This metric reflects how consistently the system produces a valid interaction given specific constraints such as classification algorithm.

Signal quality (spatial accuracy) of the interaction: For each simulated interaction, we compute the spatial accuracy as the angular offset between the centroid of the fixation and the corresponding target center, measured in dva:

$$\theta = \frac{180}{\pi} \arccos \left(\frac{G \cdot T}{\|G\| \|T\|} \right) \quad (12)$$

where G is the gaze centroid vector and T is the target vector.

To evaluate performance across participants, spatial accuracy is summarized using both user-level and population-level percentiles following [57]:

$E50$: Median error for an individual user.

$E95$: 95th percentile error for an individual user.

$U50|E50$: Median of $E50$ values across all users (population-level).

$U95|E95$: 95th percentile of $E95$ values across users (worst-case population-level).

4 RESULTS

Table 1 presents a comparative analysis of several lightweight privacy-preserving approaches applied to the dataset, focusing on the trade-off between privacy and gaze-interaction utility. Privacy is represented by the Rank-1 IR, which reflects how easily a user can be re-identified from gaze data. A lower IR indicates stronger privacy. Utility, on the other hand, is assessed through spatial accuracy metrics under two eye movement classification algorithms— IDT and IKF— where smaller error values ($U50|E50$, $U95|E95$) and higher success rates (SR%) correspond to better performance. Additionally, the table reports each approach’s initialization delay and the latency introduced during real-time processing.

Baseline raw data achieves the highest Rank-1 IR (96.61%) with an excellent interaction definition success rate. But the highest Rank-1 IR also brings the highest risk of user re-identification. This underscores the inherent privacy vulnerability of unmodified gaze data.

Applying a median filter slightly reduces re-identification accuracy (to 94.92 %, lowering the Rank-1 IR by about 2% less than the baseline case) while maintaining nearly identical utility and negligible latency (1 ms), indicating that lightweight smoothing offers modest privacy gains without harming performance.

Temporal sampling demonstrates a progressive reduction in identifiability as sampling frequency decreases, with Rank-1 IR dropping from 92.98% at 500 Hz to 52.63% at 100 Hz. The utility measures for both IDT and IKF improve. The $U95|E95$ metric goes down, indicating better performance with a lower sampling rate. We have to remember that the number of samples drastically reduced from 1000 Hz to lower sampling frequencies like 100 or 50 Hz. With a higher number of factors for the decimation, it brings a higher initialization delay in the process.

Linearly weighted average smoothing with wider temporal windows (50–200 samples) yields moderate privacy gains (Rank-1 IR \approx 88–86%, 8–10% less than the baseline case) while maintaining great spatial accuracy across user and population-level. The highest success rate in defining interaction indicates that the maximum number of interactions is counted in the calculation of spatial accuracy. But it is achieved at the cost of higher initialization delay and latency (32–133 ms), and it requires a window of a certain length of data.

Gaussian noise injection produces a steeper privacy gain, though at the cost of utility. The utility measures heavily collapsed as it is unmeasurable in cases. We have not included it in the Table 1.

The targeted noise method based on 2D Laplace noise injection achieves noticeable privacy improvements (Rank-1 IR - 39.1%) while preserving other metrics. This number can be misleading because we have utilized the pretrained model from the baseline to test the noise-injected data. It is to be noted that for this approach, real-time classification of the data is required not only in defining interactions but also in the noise injection.

The Causal FIR filters achieve small privacy improvements (IR \approx 94–95%) while keeping the population level error minimum. The utility improves noticeably with this approach at the cost of latency that depends on the number of taps we use. The interaction definition success rate is also very high with this approach.

Among all tested techniques, the Kalman filter achieves one of the best overall balances. It reduces the Rank-1 IR to 88.14%, significantly lowering re-identification potential relative to the baseline, while maintaining near-baseline utility (IDT - $U_{95}|E_{95}$ = 11.8, SR \approx 99%; IKF - $U_{95}|E_{95}$ = 10.94, SR \approx 99%) and adding no measurable latency.

Table 1: Privacy–Utility Comparison. *For targeted noise addition approach the pretrained model from the baseline is used to test the noise injected data.

Approach	Variant	Rank-1 IR (%)	IDT			IKF			Initialization	Latency (ms)
			U50 E50	U95 E95	SR (%)	U50 E50	U95 E95	SR (%)		
Baseline	Raw data	96.61	0.62	12.85	99.55	0.59	13.59	97.4	0	0
Median Filter	3-sample	94.92	0.61	11.67	99.63	0.58	13.19	98.36	0	1
Temporal Sampling (Hz)	500	92.98	0.61	12.71	99.61	0.57	10.32	99.43	1	0
	250	91.22	0.60	11.32	99.68	0.57	4.48	99.94	3	0
	100	82.46	0.59	9.44	99.81	0.57	4.23	99.99	9	0
	90	82.46	0.59	9.25	99.83	0.57	3.98	99.99	10	0
	50	52.63	0.58	7.54	99.90	0.56	4.41	99.99	19	0
Smoothing (window)	50	88.14	0.61	7.84	99.86	0.55	3.9	100	49	\approx 32
	100	88.14	0.61	7.26	99.88	0.54	4.01	100	99	66
	200	86.44	0.61	6.45	99.85	0.53	4.47	100	199	\approx 133
Targeted Noise Injection*	2D Laplace	39.1	0.62	15.07	98.71	0.61	15.65	96.3	0	0
	75/79	94.92	0.62	12.62	99.68	0.57	4.88	99.98	0	39
Causal FIR (cutoff/taps)	25/49	94.92	0.61	10.99	99.78	0.56	3.87	100	0	24
	10/29	94.92	0.61	11.14	99.77	0.56	3.87	100	0	14
Kalman Filter	-	88.14	0.61	11.8	98.93	0.57	10.94	99.38	0	0

5 DISCUSSION

5.1 Privacy vs. Utility Trade-off

The results clearly demonstrate the inherent trade-off between privacy protection and utility, expressed through the spatial accuracy of gaze-based interaction. As privacy-preserving techniques are applied to raw gaze data, the ability to re-identify users decreases; however, this improvement often comes at the expense of spatial accuracy during interaction. In other words, methods that effectively obscure identity cues tend to distort gaze trajectories, thereby reducing interaction precision in real-time systems.

Certain approaches, such as Gaussian noise injection or targeted noise addition to saccadic segments, enhance privacy preservation but hamper interaction accuracy. In contrast, smoothing-based methods and FIR filtering prioritize maintaining utility by preserving the integrity of the gaze trajectory. Temporal downsampling provides a particularly illustrative case: reducing the sampling rate substantially decreases the Rank-1 Identification Rate, indicating a strong privacy benefit. However, as noted by [58], preserving lower signal frequencies up to approximately 75 Hz in the frequency domain is necessary to retain the essential characteristics of the underlying eye movement signal. Consequently, researchers must carefully determine how much gaze information can be safely discarded when sampling at 50 Hz or lower—as occurs with causal FIR filters featuring signal cut-offs around 25 Hz or 10 Hz—without compromising the validity of the recorded behavior.

Ultimately, it is the responsibility of researchers and system designers to navigate this balance - selecting techniques that enhance user privacy while retaining sufficient signal fidelity for effective and seamless interaction.

5.2 Is smoothing the key?

The implemented techniques can be broadly grouped into smoothing-based (e.g., median, Kalman, FIR filtering) and non-smoothing (e.g., temporal downsampling, Gaussian noise, targeted noise injection) approaches. While both aim to reduce person-specific patterns in gaze data, they differ in how they balance privacy and utility. Smoothing-based methods attenuate high-frequency fluctuations—often linked to individual micro-movements—without disrupting the overall gaze trajectory. In our results, Kalman, median, and FIR filters achieved moderate privacy gains with minimal degradation in spatial accuracy compared to the baseline. This indicates that smoothing regularizes the signal enough

to obscure identity cues while maintaining utility. In contrast, non-smoothing methods like noise injection improved privacy more strongly but at the cost of utility. Similarly, aggressive temporal downsampling improves privacy but reduces the effective sample size, limiting gaze resolution and responsiveness.

These findings suggest that privacy preservation in real-time gaze-based interaction systems may be most effectively achieved not through aggressive data distortion, but through lightweight but effective smoothing techniques that subtly suppress sensitive information from the gaze signal while maintaining natural gaze behavior.

5.3 Effectiveness of Filtering Approaches

Filtering-based techniques, particularly Kalman and FIR filtering, emerged as the most effective strategies for preserving both privacy and interaction utility. These filters act by modeling gaze as a continuous, temporally correlated signal, allowing noise and person-specific fluctuations to be suppressed without significantly altering gaze trajectory. Among the implemented methods, the Kalman filter provided the most balanced performance—achieving a substantial reduction in Rank-1 IR while maintaining near-baseline spatial accuracy during interaction. The FIR filter demonstrated comparable behavior, offering slightly higher latency but maintaining stable gaze continuity. Both approaches outperform static smoothing or noise-injection methods in real-time feasibility due to their adaptive and causal nature. These findings reinforce the idea that privacy in interactive gaze systems can be enhanced through dynamic signal modeling rather than random perturbation.

5.4 Implications for Real-Time Implementation

The findings highlight that the real-time applicability of lightweight privacy-preserving techniques depends critically on two system-level factors: initialization delay and latency. While many filtering methods achieved privacy improvements without major loss of spatial accuracy, their suitability for interactive use ultimately hinges on how quickly they stabilize and how efficiently they process data. Techniques such as Kalman and FIR filters require an initialization phase to estimate initial states or coefficients. Short initialization windows are acceptable for interactive systems, but longer ones can delay responsiveness, causing interaction lag. Latency, meanwhile, directly impacts user experience. Methods with minimal computational complexity—such as Kalman or median filtering—introduce negligible delay and thus maintain the immediacy essential for XR and gaze-based interfaces. In contrast, larger-window smoothing or high-tap FIR filters increase latency, which can degrade system usability along with the user experience.

These results imply that privacy mechanisms must be evaluated not only for accuracy and privacy gain but also for their temporal efficiency. In real-time applications, maintaining end-to-end delays as low as possible is vital for preserving the fluidity of interaction.

5.5 Broader Privacy Implications

Our results demonstrate that effective privacy preservation does not necessarily require heavy-handed gaze data distortion. Lightweight approaches, particularly smoothing-based filtering, can substantially reduce re-identification risk while maintaining the spatial fidelity needed for natural interaction. This finding suggests that privacy can be engineered at the signal-processing level through an efficient approach rather than relying solely on restrictive data access or post-hoc anonymization. Even when gaze data are preprocessed for privacy, residual risks remain due to the persistent identifiability of subtle behavioral traits. So, privacy must be viewed as a multi-layered responsibility—encompassing algorithmic design, system architecture, and policy governance at the same time.

5.6 Limitation and Future Research

First, although we aimed to simulate real-time conditions, the experiments relied on a publicly available offline dataset rather than live interaction data. This dataset allowed analysis over a large participant pool but may not fully capture real-time behavioral variability, such as head motion or environmental noise. Consequently, the effectiveness of certain techniques—particularly those relying on temporal dynamics—may differ in actual interactive settings.

Second, temporal downsampling is an effective way to reduce re-identification by discarding fine-grained gaze information; however, it introduces several methodological and practical limitations. The most immediate effect is a reduction in the number of gaze samples while maintaining the same recording duration. This means that temporal continuity is preserved, but the density of information within that interval is drastically lowered. Such sample reduction can create a confounded experimental condition—privacy improvements may appear to result from the downsampling itself rather than a true suppression of identity-related features. In other words, lower re-identification accuracy may stem from data sparsity rather than genuine privacy enhancement. Future research should aim to disentangle the effects of temporal downsampling from genuine privacy preservation mechanisms.

Third, while Rank-1 IR is a standard measure for evaluating re-identification risk, it is inherently dependent on the size of the subject population—larger datasets tend to produce lower Rank-1 values even when underlying identifiability remains high. Relying solely on this metric can therefore obscure true privacy performance, especially when comparing across datasets or experiments with differing subject counts.

Future studies should expand evaluation beyond real-time dataset simulation toward user-in-the-loop, real-time interaction experiments to capture the behavioral and perceptual impact of privacy-preserving techniques.

6 CONCLUSION

This study evaluated a range of real-time lightweight privacy-preserving techniques for gaze-based interaction, demonstrating that achieving privacy consistently involves a trade-off between protection strength and utility. Among the implemented techniques, smoothing-based approaches—particularly Kalman filtering proved most effective in maintaining the balance. These methods offer privacy gains through structured signal regularization rather than disruptive gaze data distortion. While temporal downsampling greatly enhanced privacy, it also reduced data richness and introduced potential confounds, underscoring that perceived privacy improvements may stem from sample sparsity rather than genuine anonymization. Real-time feasibility was found to depend primarily on processing latency, underscoring the importance of lightweight, causal implementations for interactive use. Overall, the findings indicate that privacy preservation in real-time gaze-based interaction systems, while maintaining utility, is most effectively achieved through lightweight smoothing techniques such as the Kalman filter—which reduced Rank-1 IR by approximately 8% without introducing latency. These approaches effectively suppress identity-related signal components while maintaining spatial accuracy and interaction performance.

References

- [1] Stephanie Hui-Wen Chuah. Wearable xr-technology: literature review, conceptual framework and future research directions. *International journal of technology marketing*, 13(3-4):205–259, 2019. [1](#)
- [2] Isayas Berhe Adhanom, Paul MacNeilage, and Eelke Folmer. Eye tracking in virtual reality: a broad review of applications and challenges. *Virtual Reality*, 27(2):1481–1505, 2023. [1](#)
- [3] Mehedi Hasan Raju, Samantha Aziz, Michael J Proulx, and Oleg Komogortsev. Evaluating eye tracking signal quality with real-time gaze interaction simulation: A study using an offline dataset. In *2025 Symposium on Eye Tracking Research and Applications*, ETRA '25, New York, NY, USA, 2025. Association for Computing Machinery. [1](#), [2](#), [7](#), [8](#)
- [4] Ajoy S Fernandes, T Scott Murdison, and Michael J Proulx. Leveling the playing field: A comparative reevaluation of unmodified eye tracking as an input and interaction modality for vr. *IEEE Transactions on Visualization and Computer Graphics*, 29(5):2269–2279, 2023. [1](#)
- [5] Thorsten Roth, Martin Weier, André Hinkenjann, Yongmin Li, and Philipp Slusallek. A quality-centered analysis of eye tracking data in foveated rendering. *Journal of Eye Movement Research*, 10(5):1–12, 2017. [1](#)
- [6] Rachel Albert, Anjul Patney, David Luebke, and Joohwan Kim. Latency requirements for foveated rendering in virtual reality. *ACM Transactions on Applied Perception (TAP)*, 14(4):1–13, 2017. [1](#)
- [7] Mohammed Tahri Sqalli, Begali Aslonov, Mukhammadjon Gafurov, Nurmukhammad Mukhammadiev, and Yahya Sqalli Houssaini. Eye tracking technology in medical practice: a perspective on its diverse applications. *Frontiers in Medical Technology*, 5:1253001, 2023. [1](#)
- [8] Joseph R Pauszek. An introduction to eye tracking in human factors healthcare research and medical device testing. *Human Factors in Healthcare*, 3:100031, 2023. [1](#)
- [9] R. John Leigh and David S. Zee. *The Neurology of Eye Movements*. Oxford University Press, 06 2015. [1](#)
- [10] Deborah E Hannula, Robert R Althoff, David E Warren, Lily Riggs, Neal J Cohen, and Jennifer D Ryan. Worth a glance: using eye movements to investigate the cognitive neuroscience of memory. *Frontiers in human neuroscience*, 4:166, 2010. [1](#)
- [11] Hajra Ashraf, Mikael H Sodergren, Nabeel Merali, George Mylonas, Harsimrat Singh, and Ara Darzi. Eye-tracking technology in medical education: A systematic review. *Medical teacher*, 40(1):62–69, 2018. [1](#)
- [12] Howell Istance, Stephen Vickers, and Aulikki Hyrskykari. Gaze-based interaction with massively multiplayer on-line games. In *CHI '09 Extended Abstracts on Human Factors in Computing Systems*, CHI EA '09, page 4381–4386, New York, NY, USA, 2009. Association for Computing Machinery. [1](#)

- [13] Dillon Lohr and Oleg V Komogortsev. Eye know you too: Toward viable end-to-end eye movement biometrics for user authentication. *IEEE Transactions on Information Forensics and Security*, 17:3151–3164, 2022. 1, 2, 5, 6, 7
- [14] Mehedi Hasan Raju, Lee Friedman, Dillon J Lohr, and Oleg Komogortsev. Signal vs noise in eye-tracking data: Biometric implications and identity information across frequencies. In *Proceedings of the 2024 Symposium on Eye Tracking Research and Applications*, pages 1–7, 2024. 1, 3, 4
- [15] Dillon James Lohr, Michael J. Proulx, and Oleg V. Komogortsev. Establishing a baseline for gaze-driven authentication performance in vr: A breadth-first investigation on a very large dataset. *ArXiv*, abs/2404.11798, 2024. 1, 2
- [16] Ioannis Rigas, George Economou, and Spiros Fotopoulos. Biometric identification based on the eye movements and graph matching techniques. *Pattern Recognition Letters*, 33(6):786–792, 2012. 1
- [17] Lena A Jäger, Silvia Makowski, Paul Prasse, Sascha Liehr, Maximilian Seidler, and Tobias Scheffer. Deep eye-identification: Biometric identification using micro-movements of the eye. In *Machine Learning and Knowledge Discovery in Databases: European Conference, ECML PKDD 2019, Würzburg, Germany, September 16–20, 2019, Proceedings, Part II*, pages 299–314. Springer, 2020. 1, 2
- [18] Silvia Makowski, Paul Prasse, David R. Reich, Daniel Krakowczyk, Lena A. Jäger, and Tobias Scheffer. Deep-eyedidentificationlive: Oculomotoric biometric identification and presentation-attack detection using deep neural networks. *IEEE Transactions on Biometrics, Behavior, and Identity Science*, 3(4):506–518, 2021. 1, 2
- [19] Brendan David-John, Diane Hosfelt, Kevin Butler, and Eakta Jain. A privacy-preserving approach to streaming eye-tracking data. *IEEE Transactions on Visualization and Computer Graphics*, 27(5):2555–2565, 2021. 1, 3, 4, 5
- [20] Brendan David-John, Kevin Butler, and Eakta Jain. Privacy-preserving datasets of eye-tracking samples with applications in xr. *IEEE Transactions on Visualization and Computer Graphics*, 29(5):2774–2784, 2023. 1
- [21] Ethan Wilson, Azim Ibragimov, Michael J Proulx, Sai Deep Tetali, Kevin Butler, and Eakta Jain. Privacy-preserving gaze data streaming in immersive interactive virtual reality: Robustness and user experience. *IEEE Transactions on Visualization and Computer Graphics*, 30(5):2257–2268, 2024. 2, 3, 5, 7
- [22] Pawel Kasprowski and Józef Ober. Eye movements in biometrics. In *International Workshop on Biometric Authentication*, pages 248–258. Springer, 2004. 2
- [23] Roman Bednarik, Tomi Kinnunen, Andrei Mihaila, and Pasi Fränti. Eye-movements as a biometric. In *Scandinavian conference on image analysis*, pages 780–789. Springer, 2005. 2
- [24] Corey Holland and Oleg V. Komogortsev. Biometric identification via eye movement scanpaths in reading. In *2011 International Joint Conference on Biometrics (IJCB)*, pages 1–8, 2011. 2
- [25] Ioannis Rigas and Oleg V. Komogortsev. Current research in eye movement biometrics: An analysis based on bioeye 2015 competition. *Image and Vision Computing*, 58:129–141, 2017. 2
- [26] Christina Katsini, Yasmeen Abdrabou, George E Raptis, Mohamed Khamis, and Florian Alt. The role of eye gaze in security and privacy applications: Survey and future hci research directions. In *Proceedings of the 2020 CHI conference on human factors in computing systems*, pages 1–21, 2020. 2
- [27] Sai Ganesh Grandhi. Evaluating vr/ar security through continuous authentication via eye tracking movements. Master’s thesis, University of Windsor (Canada), 2025. 2
- [28] Huafeng Qin, Hongyu Zhu, Xin Jin, Qun Song, Mounim A. El-Yacoubi, and Xinbo Gao. Emmixformer: Mix transformer for eye movement recognition. *IEEE Transactions on Instrumentation and Measurement*, pages 1–1, 2025. 2
- [29] Daniel J Liebling and Sören Preibusch. Privacy considerations for a pervasive eye tracking world. In *Proceedings of the 2014 ACM International Joint Conference on Pervasive and Ubiquitous Computing: Adjunct Publication*, pages 1169–1177, 2014. 2
- [30] Jacob Leon Kröger, Otto Hans-Martin Lutz, and Florian Müller. What does your gaze reveal about you? on the privacy implications of eye tracking. In *IFIP International Summer School on Privacy and Identity Management*, pages 226–241. Springer, 2020. 2
- [31] Vivek Nair, Christian Rack, Wenbo Guo, Rui Wang, Shuixian Li, Brandon Huang, Atticus Cull, James F O’Brien, Marc Latoschik, Louis Rosenberg, et al. Inferring private personal attributes of virtual reality users from ecologically valid head and hand motion data. In *2024 IEEE Conference on Virtual Reality and 3D User Interfaces Abstracts and Workshops (VRW)*, pages 477–484. IEEE, 2024. 2

- [32] Mariusz Wierzbowski, Grzegorz Pochwatko, Paulina Borkiewicz, Daniel Cnotkowski, Michał Pabiś-Orzeszyna, and Paweł Kobylński. Behavioural biometrics in virtual reality: To what extent can we identify a person based solely on how they watch 360-degree videos? In *2022 IEEE international symposium on mixed and augmented reality adjunct (ISMAR-Adjunct)*, pages 417–422. IEEE, 2022. 2
- [33] Mark Roman Miller, Fernanda Herrera, Hanseul Jun, James A Landay, and Jeremy N Bailenson. Personal identifiability of user tracking data during observation of 360-degree vr video. *Scientific Reports*, 10(1):17404, 2020. 2
- [34] Miao Hu, Zhenxiao Luo, Yipeng Zhou, Xuezheng Liu, and Di Wu. Otus: A gaze model-based privacy control framework for eye tracking applications. In *IEEE INFOCOM 2022-IEEE Conference on Computer Communications*, pages 560–569. IEEE, 2022. 2
- [35] Andrey V Lyamin and Elena N Cherepovskaya. An approach to biometric identification by using low-frequency eye tracker. *IEEE Transactions on Information Forensics and Security*, 12(4):881–891, 2016. 2
- [36] Efe Bozkir, Ali Burak Ünal, Mete Akgün, Enkelejda Kasneci, and Nico Pfeifer. Privacy preserving gaze estimation using synthetic images via a randomized encoding based framework. In *ACM symposium on eye tracking research and applications*, pages 1–5, 2020. 2
- [37] Yang Wang. Privacy-enhancing technologies. In *Handbook of research on social and organizational liabilities in information security*, pages 203–227. IGI Global Scientific Publishing, 2009. 2
- [38] Arvind Narayanan and Vitaly Shmatikov. Robust de-anonymization of large sparse datasets. In *2008 IEEE Symposium on Security and Privacy (sp 2008)*, pages 111–125. IEEE, 2008. 2
- [39] Ao Liu, Lirong Xia, Andrew Duchowski, Reynold Bailey, Kenneth Holmqvist, and Eakta Jain. Differential privacy for eye-tracking data. In *Proceedings of the 11th ACM Symposium on Eye Tracking Research & Applications*, pages 1–10, 2019. 2
- [40] Jingjie Li, Amrita Roy Chowdhury, Kassem Fawaz, and Younghyun Kim. {Kalēido}:{Real-Time} privacy control for {Eye-Tracking} systems. In *30th USENIX security symposium (USENIX security 21)*, pages 1793–1810, 2021. 2, 5
- [41] Julian Steil, Marion Koelle, Wilko Heuten, Susanne Boll, and Andreas Bulling. Privaceye: privacy-preserving head-mounted eye tracking using egocentric scene image and eye movement features. In *Proceedings of the 11th ACM symposium on eye tracking research & applications*, pages 1–10, 2019. 2
- [42] Samantha Aziz and Oleg Komogortsev. Privacy enhancement for gaze data using a noise-infused autoencoder. *arXiv preprint arXiv:2508.10918*, 2025. 2
- [43] John Wilder Tukey et al. *Exploratory data analysis*, volume 2. Springer, 1977. 3, 4
- [44] Rudolph Emil Kalman. A new approach to linear filtering and prediction problems. 1960. 3
- [45] Oleg V Komogortsev and Javed I Khan. Kalman filtering in the design of eye-gaze-guided computer interfaces. In *International Conference on Human-Computer Interaction*, pages 679–689. Springer, 2007. 3
- [46] Mehedi H Raju, Lee Friedman, Troy M Bouman, and Oleg V Komogortsev. Filtering eye-tracking data from an eyelink 1000: Comparing heuristic, savitzky-golay, iir and fir digital filters. *Journal of Eye Movement Research*, 14(3):10–16910, 2023. 3, 5
- [47] Henry Griffith, Dillon Lohr, Evgeny Abdulin, and Oleg Komogortsev. Gazebase, a large-scale, multi-stimulus, longitudinal eye movement dataset. *Scientific Data*, 8(1):184, 2021. 3
- [48] Dillon Lohr, Henry Griffith, and Oleg V Komogortsev. Eye know you: Metric learning for end-to-end biometric authentication using eye movements from a longitudinal dataset. *IEEE Transactions on Biometrics, Behavior, and Identity Science*, 2022. 6
- [49] Gao Huang, Zhuang Liu, Laurens Van Der Maaten, and Kilian Q Weinberger. Densely connected convolutional networks. In *Proceedings of the IEEE conference on computer vision and pattern recognition*, pages 4700–4708, 2017. 6
- [50] Diederik P Kingma and Jimmy Ba. Adam: A method for stochastic optimization. *arXiv preprint arXiv:1412.6980*, 2014. 6
- [51] Leslie N Smith and Nicholay Topin. Super-convergence: Very fast training of neural networks using large learning rates. In *Artificial intelligence and machine learning for multi-domain operations applications*, volume 11006, pages 369–386. SPIE, 2019. 6
- [52] X. Wang, X. Han, W. Huang, D. Dong, and M. R. Scott. Multi-similarity loss with general pair weighting for deep metric learning. In *2019 IEEE/CVF Conference on Computer Vision and Pattern Recognition (CVPR)*, pages 5017–5025, 2019. 6

- [53] Kevin Musgrave, Serge Belongie, and Ser-Nam Lim. Pytorch metric learning, 2020. [6](#)
- [54] Dario D Salvucci and Joseph H Goldberg. Identifying fixations and saccades in eye-tracking protocols. In *Proceedings of the 2000 Symposium on Eye Tracking Research & Applications*, New York, NY, USA, 2000. Association for Computing Machinery. [7](#)
- [55] Do Hyong Koh, Sandeep A. Munikrishne Gowda, and Oleg V. Komogortsev. Input evaluation of an eye-gaze-guided interface: kalman filter vs. velocity threshold eye movement identification. In *Proceedings of the 1st ACM SIGCHI Symposium on Engineering Interactive Computing Systems*, EICS '09, page 197–202, New York, NY, USA, 2009. Association for Computing Machinery. [7](#)
- [56] Lee Friedman, Ioannis Rigas, Evgeny Abdulin, and Oleg V Komogortsev. A novel evaluation of two related and two independent algorithms for eye movement classification during reading. *Behavior Research Methods*, 50:1374–1397, 2018. [7](#)
- [57] Samantha Aziz, Dillon J Lohr, Lee Friedman, and Oleg Komogortsev. Evaluation of eye tracking signal quality for virtual reality applications: A case study in the meta quest pro. In *Proceedings of the 2024 Symposium on Eye Tracking Research and Applications*, ETRA '24, New York, NY, USA, 2024. Association for Computing Machinery. [8](#)
- [58] Mehedi H Raju, Lee Friedman, Troy M Bouman, and Oleg V Komogortsev. Determining which sine wave frequencies correspond to signal and which correspond to noise in eye-tracking time-series. *Journal of Eye Movement Research*, 14(3):16, 2023. [9](#)